

Study of Short Cracks Growth Behavior for Duralumin 7075-T₆ Enhanced by Artificial Ageing as Thermal and Chemical Treatments Under Rotating Bending Loading

Dr. Mustafa Sami Abdullateef

Electromechanical Engineering Department, University of Technology/Baghdad
mustafaalshaker@yahoo.com

Received on: 30/1/2013 & Accepted on: 9/5/2013

Abstract

The fatigue life of ductile metals is controlled mainly by the propagation life of a short surface crack; to clarify the growth behavior of short cracks is crucial factor to the safe design of smooth surface members. However, little has been reported on the growth behavior of short surface cracks in thermal-chemical treated duralumin. In the present study, stress-controlled fatigue tests (under rotating bending load) for 70 hours artificial aged duralumin 7075-T₆ without chemical treatment case (1) and with chemical treatment case (2). The growth behavior of short cracks was monitored by a plastic replication technique and the surface damage (short crack propagation) during cyclic stressing was observed by optical microscopy. The physical background of fatigue damage for case (1) and case (2) was discussed from the viewpoints of the initiation and growth behavior of short cracks.

Keywords: Duralumin 7075-T₆, Artificial ageing, Short cracks, Crack growth, Plastic replication technique.

دراسة تصرف نمو الشقوق القصيرة لسبيكة الديورلومين 7075-T₆ المحسنة بالتعتيق الصناعي وبالعمليات الحرارية والكيميائية تحت حمل الأحناء الدوراني

الخلاصة

يتم التحكم بعمر الكلال للمعادن المطيلية عن طريق عمر امتداد (إنتشار) شقوق السطح القصيرة، حيث ان التوضيح الوافي لتصرف نمو الشقوق الصغيرة يكون عاملاً حاسماً في التصميم الآمن للأجزاء ذات السطوح الملساء. هناك القليل من البحوث التي تم التطرق فيها الى وصف تصرف شقوق السطح القصيرة في سبائك الديورلومين المعاملة حرارياً وكيميائياً. في هذا البحث تم إجراء فحص الكلال ذات الأحماد المسيطر عليه (تحت حمل الأحناء الدوراني) لسبيكة الديورلومين 7075-T₆ ذات التعتيق الصناعي ولمدة زمنية تصل الى 70 ساعة وبدون معاملة كيميائية، (الحالة 1)، وبالمعاملة الكيميائية (الحالة 2) وذلك لغرض مراقبة نمو الشقوق القصيرة بواسطة تقنية الطبعة البلاستيكية، حيث تم رصد امتداد (إنتشار) الشقوق القصيرة أثناء الأجهادات الدورية عن طريق مايكروسكوب بصري. وتم أيضاً مناقشة الخلفية الفيزيائية للضرر الناتج من الكلال للحالة 1 و 2 من وجهة نظر تصرف نشوء ونمو الشقوق القصيرة.

٢١٦٦

<https://doi.org/10.30684/etj.31.11A12>

2412-0758/University of Technology-Iraq, Baghdad, Iraq

This is an open access article under the CC BY 4.0 license <http://creativecommons.org/licenses/by/4.0>

Introduction:

Aluminum alloys have been the primary material of choice for structural components of aircraft since about 1930. The Duralumin has a dominant in the structure of aircraft to some extent where most of the plates and rivets are manufactured from the 2024 and 7075 aluminum alloys. F.A. Al-Shamma [1] carried out the effect of combined buckling shear and bending stresses on the crack propagation. The analytical solution is based on a combination of maximum strain under mixed mode. Different boundary conditions are included in the flat plates, and new stress intensity factors for combined modes I and II have been developed for the crack growth. Also the results show the effect of crack length on the stress distribution and the direction of crack propagation. D.R.Tadjiev et al. [2] studied the fatigue crack growth prediction under random loading in specimens of high strength aluminum alloy using modified root mean square (RMS) model for each specimen to determine the max. and min. stresses under constant amplitude loading. R.Doglione and M. Bartolone [3] studied the fatigue crack propagation in a 2195-T₈ alloy plate. They showed that fatigue resistance of this alloy is comparable to that of the classical competitor alloys and high lights stress ratio (R) effects on the behavior at the threshold which causes the stress intensity range (ΔK_{th}) decrease as (R) increases. Dariusz R. and Ewald M.[4] present the static and cyclic properties of aluminum alloy AlCu4Mg1 and test the results of fatigue crack growth in plane notched specimens under bending and proportional bending with torsion. Mustafa S. A. et al.[5] showed the ageing process were used for duralumin 7075-T₆ as a major heat treatment method without case(1) and with chemical treatment case(2). The experimental results revealed that mechanical properties of selective alloy were significantly changed by case(2). By increasing the ageing time interval, hardness and ultimate tensile strength are gradually increasing and ductility was decreased. Moreover, rather interesting condition is observed in endurance limit for zero mean stress ($R = -1$) at room temperature for each time interval improved in case(2) in return for case(1).

In the present work, the stress controlled fatigue test for artificial aged duralumin 7075-T₆ with 70 hour aging time, without case(1) and with case(2) chemical treatment, were conducted to study the crack growth behavior of a short cracks that monitored by using a plastic replication technique (PRT). The physical background of fatigue damage was discussed from the viewpoints of the initiation and growth behavior of short cracks.

Experimental Procedure for Specimens Preparation:

- **Material Preparation:**

The material used in this study was Alloy 7075-T₆ has been thoroughly evaluated for corrosion resistance of atmospheric weathering, stress- cracking and exfoliation in all currently available tempers. T₆ solution heat-treated and then artificially aged. Prerequisites for hardening—small, optimally dispersed precipitates have been suggested by the previous two paragraphs. A recipe for hardening an Al-4 wt% Cu alloy therefore necessitates the following steps:

1. **Solution** heat-treat to solution temperature (T) (e.g., 520°C) in the α phase field.
2. **Quench** to a low temperature (e.g., 25°C) in the α field.

3. **Anneal** or **age** at temperature (185°C) by immersing the specimens in sulphuric acid with condensation (35%),[6] for the time necessary to optimally form coherent θ' phase precipitates and develop maximum mechanical properties. Two cases are studied in present work as follows:

Case (1): Solution → Quench → aging(70 hour) without chemical treatment.

Case (2): Solution → Quench → aging(70 hour) with chemical treatment (immersing the specimens in sulphuric acid with condensation (35%)). Note that however, duralumin are usually cooled rapidly from the quenching temperature to relatively low temperatures (25°C) and then tempered immediately to prevent cracking [5].

- **Specimens Preparation:**

Round bar specimens of 25 mm diameter ,Figure(1), were machined from the annealed processed bars (rolled round bars of 25mm in diameter and 6m in length). Before testing, all the specimens were electropolished to remove about 25 μm from the surface layer in order to facilitate observations of the surface state.

All tests were carried out at room temperature using a rotating bending fatigue machine operating at 3000 rev/min. The surface damage (crack initiation) during cyclic stressing was observed by optical microscopy. The measurement of crack length was conducted using a PRT. The crack length, l , is a length measured along the circumferential direction of the surface. The stress value referred to in this paper is that of the nominal stress amplitude, σ_a , at the minimum cross-section.

- **Microstructure and Mechanical Properties of the Materials**

Figure (2) shows typical microstructures for case(1) and case(2) material. Grain size of case(1) was about 100 μm . For case(2), refinement of structure is evident. Namely, granular grains with average size of 300 μm are formed, and grain boundary (GB) areas involve a high population of dislocations. The SADP (selected area diffraction patterns of the center area, 1 μm in diameter) consists of rings of diffraction spots, showing that GBs have high angles of misorientation. In addition, the GBs had lost their sharpness and exhibited a 'spotty' contrast and broad contours, suggesting non-equilibrium GBs contain random networks of GB dislocations [6]. Figure(2) illustrated the microstructural view for 70 hour aging time with and without immersing in sulphuric acid (35%). Samples of optical microscopes observation were mechanically polished and etched with mixed acid (1%Hf + 1.5%HCl + 2.5%HNO₃ + H₂O), and the observation, analysis and photograph were done in optical microscope (NEOPHPT-33). The existing states and it effects of trace of Sulfur (S) on the microstructure were investigated using the electron microscope (SEM) (HITACHI S-3500N). Table (1) shows the chemical analysis of the case1 and case(2) that obtained from inspection processes that take placed Specialized Institute for Engineering Industries of Iraq (SIEI). The mechanical properties of case1 were 532 MPa tensile strength, 11% elongation, and a Brinell hardness number(HRB) number of 125. After chemical treatment, case(2), their value changed to 591 MPa, 10.5, and 158, respectively, as shown in Table (2) [5].

Figures (3-a) and (3-b) show the postfracture surface for tensile specimens of case1 and case(2), respectively. The fracture surface of case(1) shows many dimples. The case(2) shows a flat fracture surface, including a couple of dimples, compared to

the fracture surface of case(1). There is no significant difference in the dimple size between two samples, in spite of the two orders of magnitude difference in grain size. Nevertheless, the dimples are shallower for the case2 because of its decreased ductility.

Plastic Replication Technique (PRT):

The replication material – G255 is cellulose acetate sheets of thickness 35 micron (0.0014 inch) that soluble in acetone. The following procedure to explain the usage of this material to replicate the surface of tested specimens. A piece of the replica material of size suitable to cover the area to be replicated is cut from the sheet. A drop or two of acetone is placed on to the specimen surface and the replica film immediately applied (allowing surface tension forces to pull it down; no pressure is required). The film should be left to dry for about 10 minutes, then it will separate very easily from any reasonably flat surface.

It can then be stretched between two pieces of cellulose tape, structure side outwards, wrapped round a microscope slide, as shown in figure(4). The required area is cutout from the film, and laid on the microscope grids on a wire mesh standing in a dish of acetone with the acetone just touching the bottom of the mesh. After one hour, remove the grids from the mesh and wash individually in acetone before drying[7].

Formation Behavior of Fatigue Damage:

Figure (5) shows the S-N curve of case(1) and case(2) material. For case(2) examined under stress controlled testing, the enhancement in fatigue life is obvious, [5]. The degree of enhancement is sharply increased with increasing stress amplitude. In the long-life field in excess of $N = 10^8$ cycles. Figure (6) shows initial growth behavior from a major crack, which led to the final fracture of the specimen, monitored by PRT. At an early stage of cycling, for case1, slip bands were formed within a grain. A grain size crack was initiated from slip bands at an about 20% of fatigue life. For case2, a 30 μ m length crack was initiated at about 20% of fatigue life.

Results and Discussion:

Figures (7-16) shows the crack growth curve ($\ln l$ vs. N relation). The relationship for case(2) can be approximated by a straight line independent of stress amplitude. For case(1), however, the relationship depends on stress amplitude. Namely, the growth curves at a stress above $\sigma_a = 100$ MPa are nearly represented by a straight line. At a stress below $\sigma_a = 100$ MPa, a linear relation of the growth curve nearly holds for a crack length in excess of $l = 0.3$ mm, whereas, each plot for $l < 0.3$ mm deviates upward from an extension of the linear relation for $l > 0.3$ mm.

The linear relation shown in figures (7-16) means that crack growth rate (CGR, dl/dN) should be proportional to l at constant stress amplitude. Figures (17-28) shows the CGR versus crack length relation. The CGR for case(1), figures(17-22) is nearly proportional to the crack length ($dl/dN \propto l$) with the exception of the CGR below $dl/dN = 10^{-6}$ mm/cycle. For case(2), figures(23-28), the $dl/dN \propto l$ relation nearly holds even for extremely low CGR range ($dl/dN < 10^{-6}$ mm/cycle) in spite of some fluctuating plots around $dl/dN = 10^{-8}$ mm/cycle. The comparison of the relation at $\sigma_a = 120$ MPa for both cases(1 & 2) indicates that CGR of case(1) is about three times larger than that of case(2). In

addition, relation at 80 MPa for case(1) is nearly equivalent to that at 85 MPa for case(2). These are different from the growth behavior of other temper of Al alloys, in which finer microstructures exhibit higher growth rates [8]. This means that applied stress amplitudes were sufficiently short and a crack propagated under the small scale yielding condition. In the present fatigue tests, the stress amplitudes were excessively large compared to stresses applied to other alloys. For case(1), especially, the ratios of stress amplitude to tensile strength, $\sigma_a/0.5\sigma_u$, were 0.28 and 0.41 for $\sigma_a = 80$ and 120 MPa, respectively. Accordingly, the crack at $\sigma_a = 120$ MPa propagates under high scale yielding, showing accelerated CGR compared to case2 with higher tensile strength. The dependency of CGR on stress amplitude was studied and it showed that dl/dN is nearly proportional to (σ_a^n) at a constant crack length. The value of n was about 7.9 and 4.8 for case(1) and case(2) Al alloys, respectively [9]. Considering the stress dependency and the relation ($dl/dN \propto l$) in figures (17-28) together, thus, the CGR of the present cases is uniquely determined by a term $\sigma_a^n l$, namely short-crack growth law (SCGL) defined by equation (1) holds, [10];

$$\frac{dl}{dN} = C_1 \sigma_a^n l \quad \dots \dots (1)$$

Where; C_1 is a constant of metals.

Figures (29 &30) ,for case(1) and case(2) respectively, shows the dl/dN versus $\sigma_a^n l$ relation. It is evident that the SCGL is available for estimating CGR of a short surface crack propagating with a growth rate above 10^{-6} and 10^{-7} (mm/cycle) for case(1) and case(2), respectively.

Many researchers have reported that the growth rate of fatigue cracks can be unified in terms of the stress intensity factor range ΔK . Here, the parameter ΔK is the effective parameter for a crack when the condition of small scale yielding at a crack tip is satisfied. The value of ΔK for an infinite plate with a crack is given by the following equation[11]:

$$\Delta K = \Delta\sigma (\pi a)^{1/2} \quad \dots \dots (2)$$

This equation indicates that the stress range has to be higher for a short crack in order to get the same growth rate as for a larger crack. Therefore, when a sufficiently short crack propagates at a finite growth rate (for example, 10^{-6} to 10^{-3} mm/c) the condition of small scale yielding is not usually satisfied. Thus the growth rate of a short crack cannot be determined uniquely by ΔK . Nisitani and Goto[8] showed that a term $(\sigma_a^n l)$ is effective parameter to determine the CGR of a short crack in many ductile materials. Here, n is a material constant. The expression $\sigma_a^n l$ ($n = 3$) was first proposed by Frost and Dugdale [12]. They applied it to comparatively large cracks in which the condition of small scale yielding nearly holds. Now $\sigma_a^n l$ can be considered as an approximation for ΔK , whereas $\sigma_a^n l$ in the present study is a parameter for crack propagation under large scale yielding. Moreover, an effective and convenient method based on a SCGL in which the effect of mechanical properties is considered has been proposed for predicting the fatigue life of smooth surface members of many annealed metals [13]. The prediction was in good agreement with the experimental results. Thus, Figure(30) means an applicability of SCGL to the evaluation of fatigue life of fine grain metals.

Conclusions:

The main results of the present study can be summarized as follows:

- (1) At a high stress amplitude ($\sigma_a > 100$ MPa), growth rate of a small crack of case(1) Al alloy was larger than that of case2 Al.
- (2) At $\sigma_a = 80$ MPa, however, CGR of case(1) was nearly equivalent to that of case(2). In case(1), the ratio of $\sigma_a = 100$ MPa to tensile strength was about 0.572. In a range of $\sigma_a > 100$ MPa, thus, the crack in case(1) propagates under large scale yielding, showing accelerated CGR compared to case(2) with higher tensile strength.
- (3) The growth rate of a short crack cannot be unified in terms of the stress intensity factor range ΔK , but it was uniquely determined by a term ($\sigma_a^n l$). Here, n is a material constant and the value of n was about 7.9 and 4.8 for case(1) and case(2) Al alloys, respectively.
- (4) For case(1) Al alloy, the term could estimate the growth rate of a crack propagating with $dl/dN > 10^{-6}$ mm/cycle. For case(2), the term was applicable to a crack with an extremely low growth rate ($dl/dN > 10^{-7}$ mm/cycle).

References

- [1] Fathi A. A., "The Effect of Fatigue on Crack Propagation in Flat Plates under Buckling Bending and Shear", Jordan Journal of Mechanical and Industrial Engineering, Volume 3, Number 3, September 2009.
- [2] D.R. Tadjive, S.T. Ki, "Fatigue crack growth prediction in 7475-T⁷³⁵¹ Aluminum Alloy under Random loading using modified root mean square model", Yeungman university, South korea, 2003.
- [3] Zhu, Y.T. & Lowe, T.C., "Observations and issues on mechanisms of grain refinement during ECAP process", *Mater Sci Eng*, A291, pp.46-53, 2000.
- [4] Dariusz R. and Ewald M., " Crack Growth in AlCu4Mg1 Alloy under Combined Cyclic Bending and Torsion", Opole University of Technology, Publisher InTech www.intechopen.com, Poland, 2011
- [5] Mustafa S. Abdullateef, Muhannad Z. K., Yasser A. M., Hayder M. A., " Enhancement of the Mechanical Properties and Fatigue Behavior for Duralumin 7075-T₆ by artificial ageing with and without chemical treatment by precipitation mechanism", Anbar Journal for Engineering Sciences, vol.1, Iraq, 2013.
- [6] Chung, C.S., Kim, J.K., Kim, H.K. & Kim, W.J., " Correlation between the nanomechanical properties and microstructure of ultrafine grained duralumin produced by equal channel angular pressing", *Mater Sci Eng*, A396, pp.11-21, 2005.
- [7] Instruction manual of replication material – G225, Agar Scientific Ltd company, England, 2011.
- [8] Chung, C.S., Kim, J.K., Kim, H.K. & Kim, W.J., "Improvement of highcycle fatigue life in a 6061Al alloy produced by equal channel angular pressing", *Mater Sci Eng*, A337, pp. 39-44, 2002.
- [9] Nisitani, H. & Goto, M., (Eds: Miller, K.J. & de los Rios, E.R.), " A small- Crack Growth Law and its Application to the Evaluation of Fatigue Life. *The behaviour of short fatigue cracks*", Mech Eng Publications Lim: London pp.461-478, 1986.

- [10] Nisitani, H., "Unifying treatment of fatigue crack growth laws in small, large and nonpropagating cracks", Mechanics of Fatigue -AMD(Ed: Mura, T.), ASME, 43, pp.151-166, 1981.
- [11] Goto, M., Han, S.Z., Kim, S.S., Ando, Y. & Kawagoishi, N., "Growth mechanism of small surface-crack of ultrafine grained copper in a highcycle fatigue regime" *Scripta Mater*, 2009.
- [12] Forst, N.E. & Dugdale, D.S., "the propagation of fatigue cracks in sheet specimens", J. Mechanics & Physics Solid, 6, pp.92-110, 1958.

Case	Cu	Mg	Mn	Si	Fe	Cr	Zn	Ti	S	Al
1	2.6	2.2	0.28	0.23	0.4	0.21	5.7	0.18	---	Reminder
2	2.49	2.08	0.287	0.23	0.41	0.19	5.2	0.2	0.13	Reminder

- [13] Goto, M. & Nisitani, H., "Inference of a small cracks growth law based on the S-N curves", Trans Jpn Soc. Mech. Eng., A56, 1990.

Yield Strength		Tensile strength		Hardness(HRB)		Elongation	
Case1(MPa)	Case2(MPa)	Case1(MPa)	Case2(MPa)	Case1	Case2	Case1	Case2
503	532	572	591	125	158	11	10.1

Table (1) Chemical composition of case(1) and case(2) duralumin 7075-T₆.

Table (2) Mechanical properties of case(1) and case(2) duralumin 7075-T₆ [5].



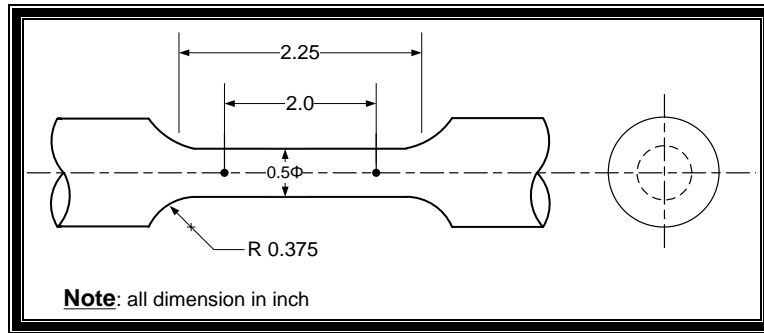
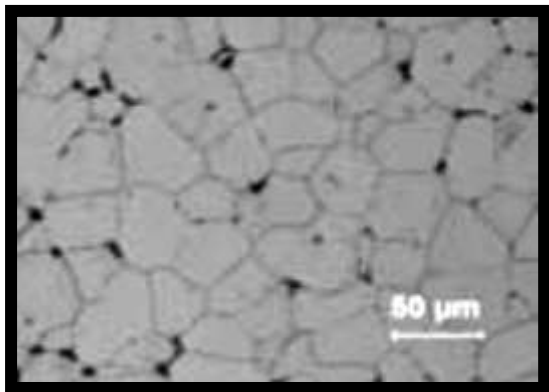
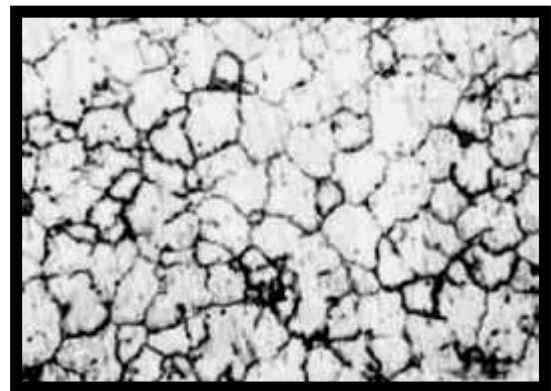


Figure (1) Fatigue Test Specimen[5]



Case(1)



Case(2)

Figure (2) microstructural of case (1) and case (2) with 70 hours of ageing[5].

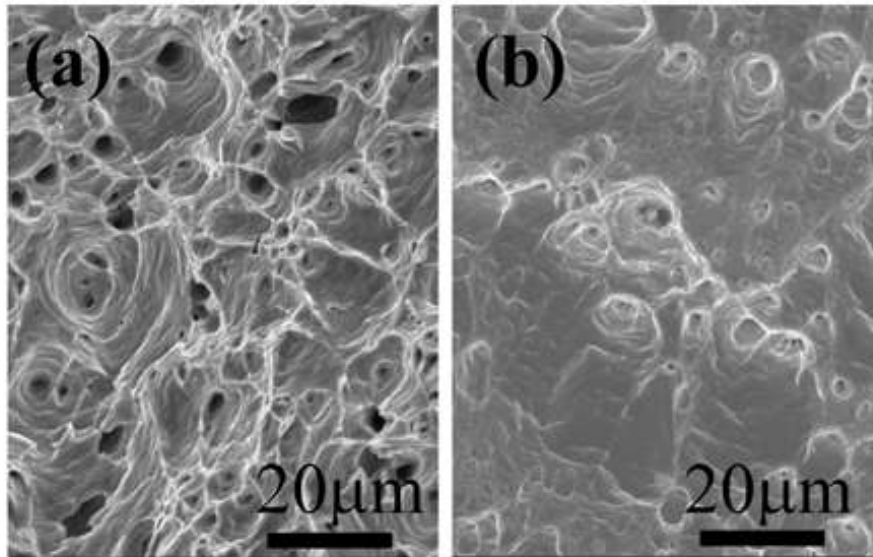


Figure (3) Fracture surface of tensile specimens; (a) case(1), (b) case(2)



Figure (4) microscopic slide of plastic replication technique



No. of cycles (<i>N</i>) (cycle)	Case (1)	No. of cycles (<i>N</i>) (cycle)	Case (2)
---------------------------------------	----------	---------------------------------------	----------

Figure (5) S-N curve of 7075-T₆ under rotating bending loading with zero mean stress for 70hours aging time[5]

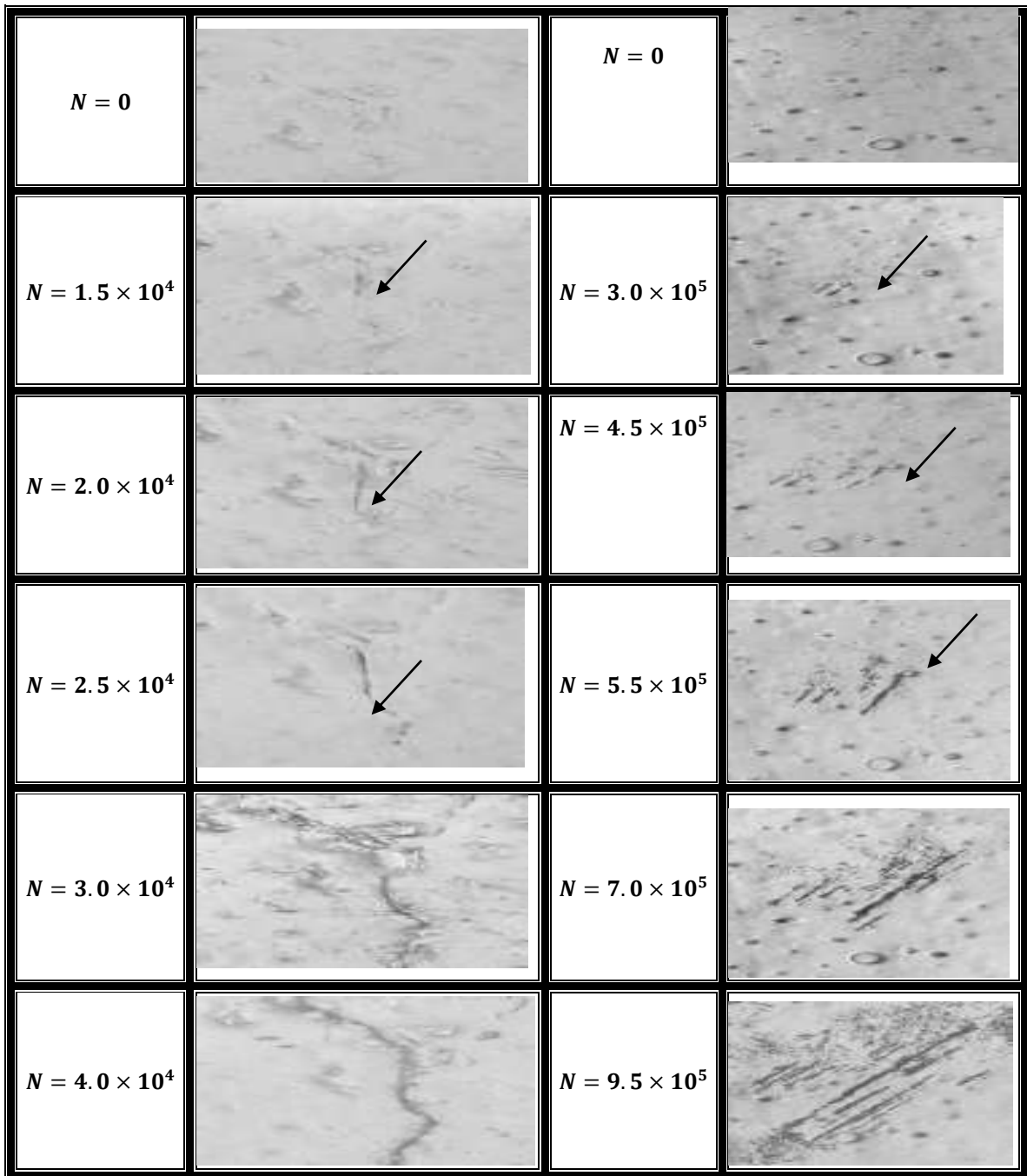
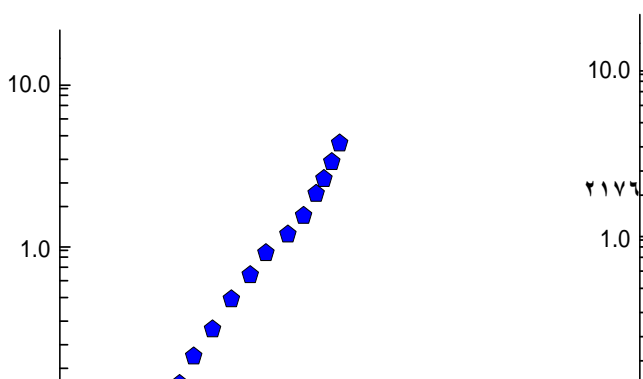


Figure (6) The surface state around a major crack observed by a plastic replication technique for case(1) $\sigma_a = 120MPa$, $N_f = 2.788 \times 10^6$, and case(2) $\sigma_a = 120MPa$, $N_f = 1.061 \times 10^7$



Crack length l (mm)

Crack length l (mm)

Figure.(7) Crack growth curve ($\log l$ vs N) Case(1) at stress amplitude $\sigma = 130$ MPa

Figure.(8) Crack growth curve ($\log l$ vs N) Case(1) at stress amplitude $\sigma = 120$ MPa

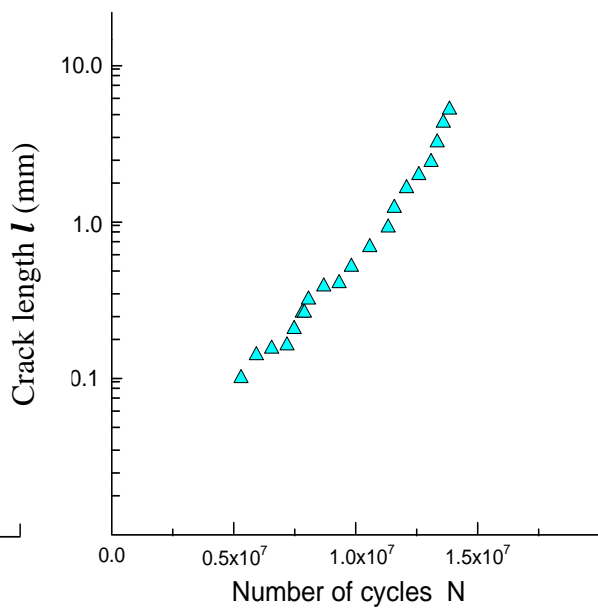
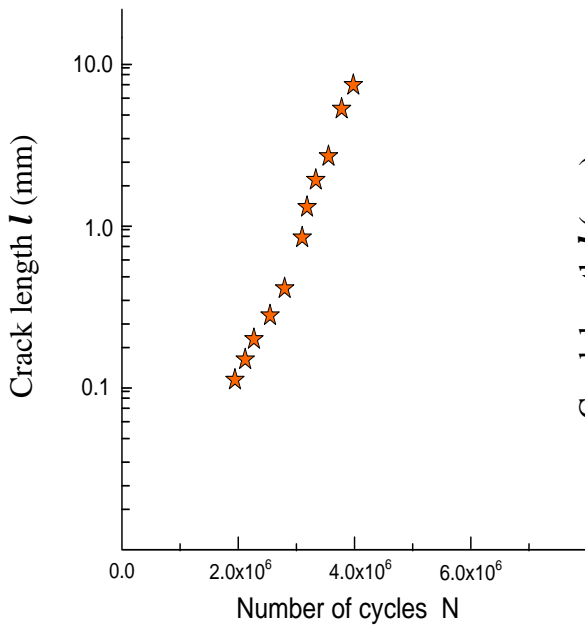
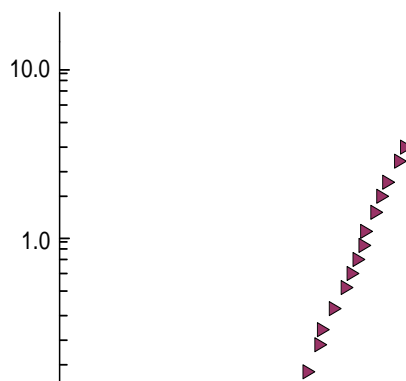
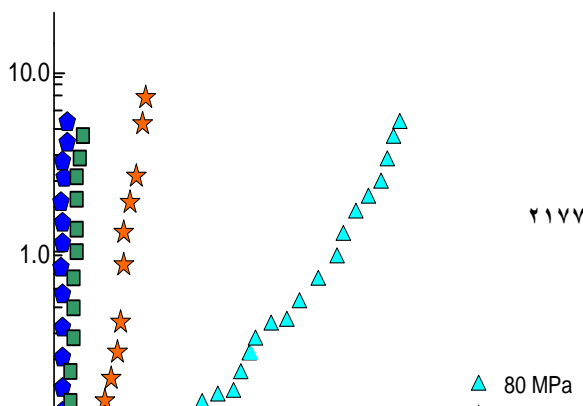


Figure.(9) Crack growth curve ($\log l$ vs N) Case(1) at stress amplitude $\sigma = 100$ MPa

Figure.(10) Crack growth curve ($\log l$ vs N) Case(1) at stress amplitude $\sigma = 80$ MPa



Crack length l (mm)

Crack length l (mm)

Figure.(11) Crack growth curves ($\log l$ vs N) relation Case(1)

Figure.(12) Crack growth curve ($\log l$ vs N) Case(2)

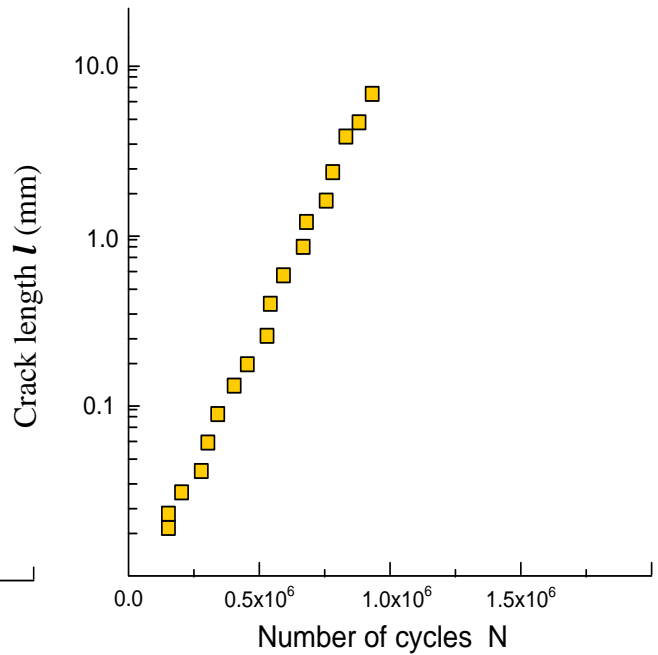
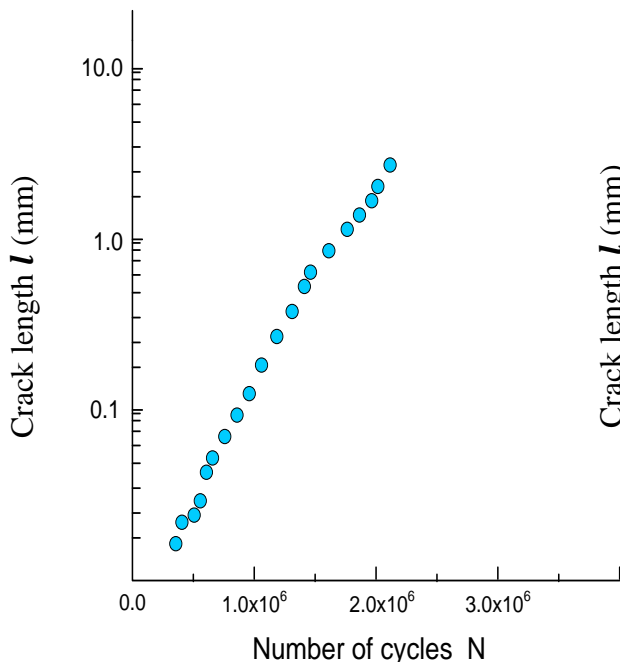


Figure.(13) Crack growth curve ($\log l$ vs N) Case(2) at stress amplitude $\sigma = 120$ MPa

Figure.(14) Crack growth curve ($\log l$ vs N) Case(2) at stress amplitude $\sigma = 160$ MPa

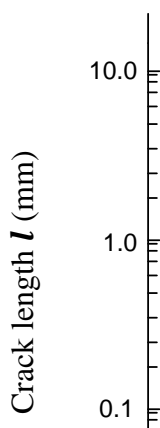


Figure.(15) Crack growth curve ($\log l$ vs N) Case(2) at stress amplitude $\sigma = 200$ MPa

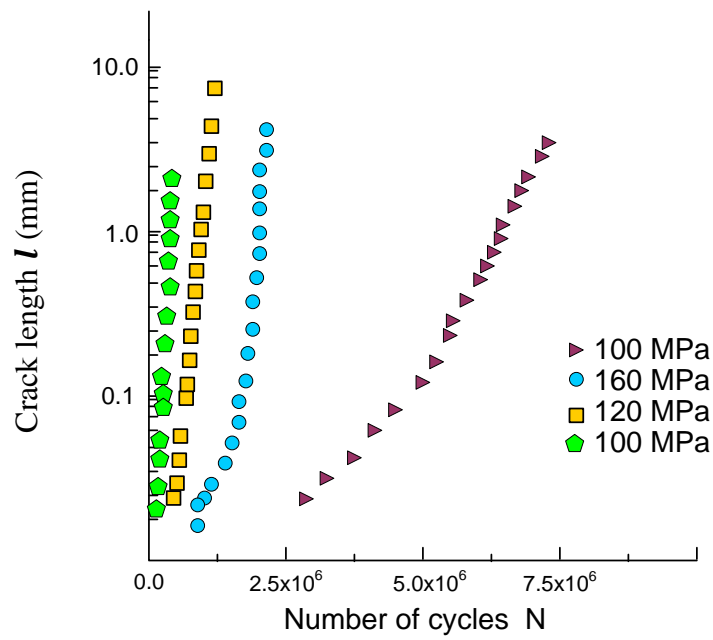
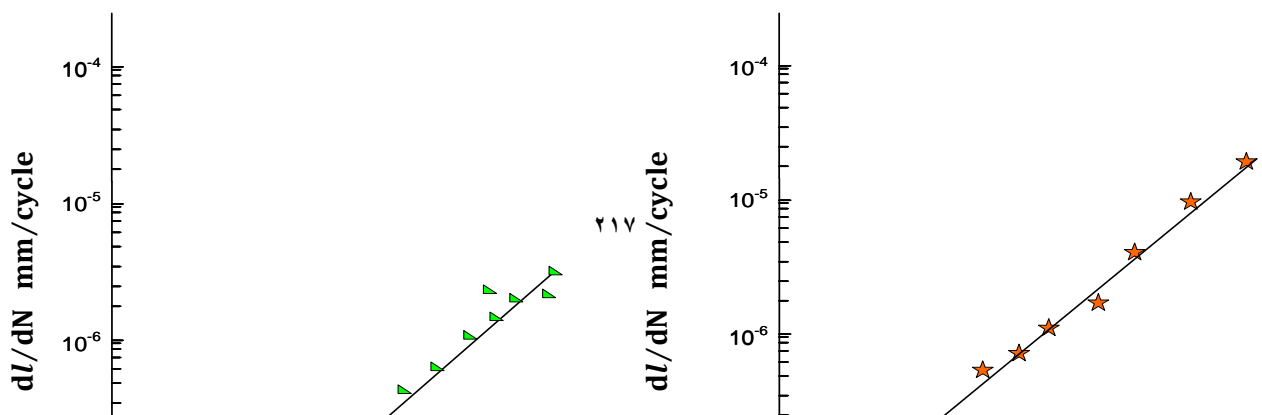
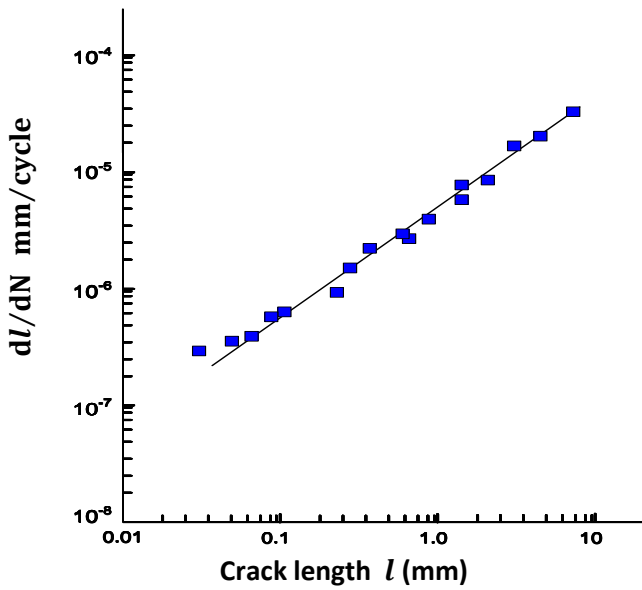


Figure.(16) Crack growth curve relation ($\log l$ vs N) Case(2)



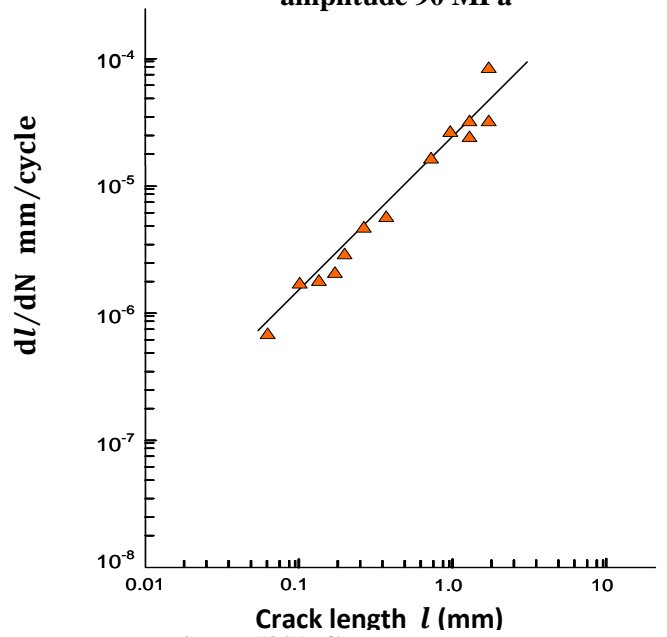
Crack length l (mm)

Figure.(17) Crack growth data (dl/dN vs l relation), Case(1), under stress amplitude 80 MPa



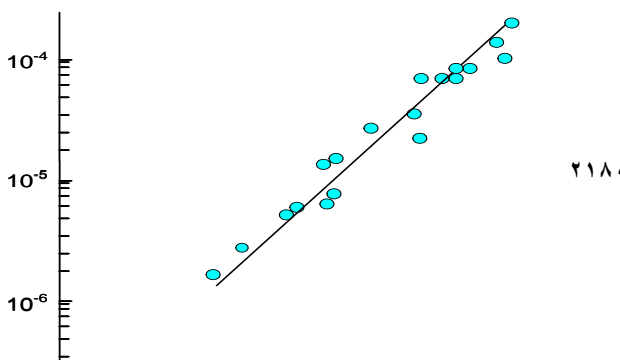
Crack length l (mm)

Figure.(18) Crack growth data (dl/dN vs l relation), Case(1), under stress amplitude 90 MPa



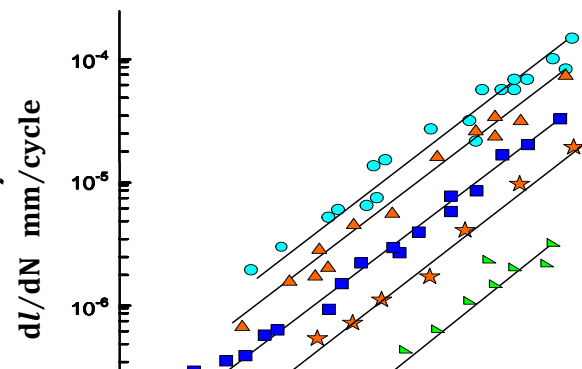
Crack length l (mm)

Figure.(19) Crack growth data (dl/dN vs l relation), Case(1), under stress amplitude 100 MPa



Crack length l (mm)

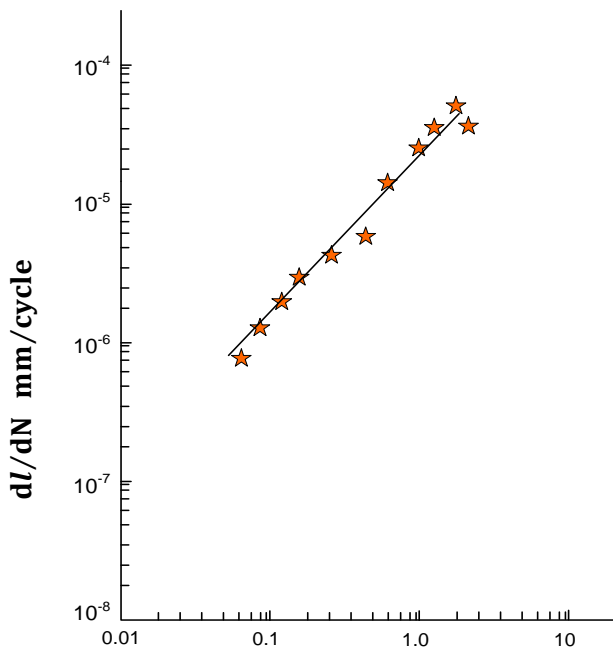
Figure.(20) Crack growth data (dl/dN vs l relation), Case(1), under stress amplitude 120 MPa



dl/dN mm/cycle

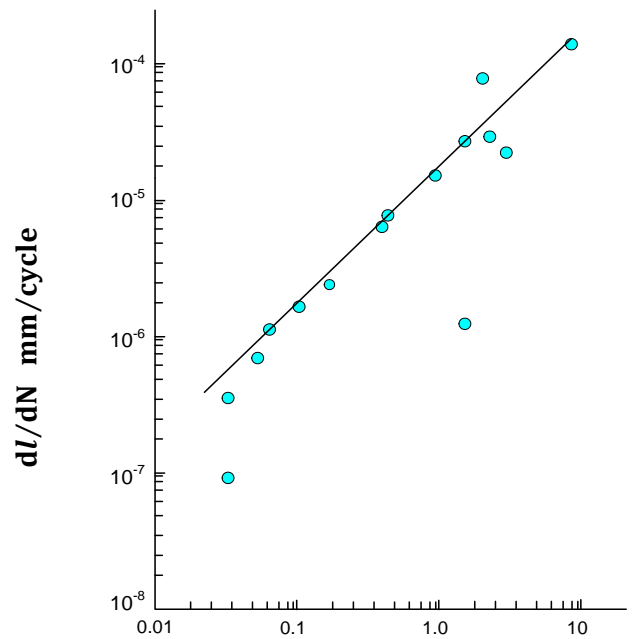
Crack length l (mm)

Figure.(21) Crack growth data (dl/dN vs l relation), Case(1), under stress amplitude 130 MPa



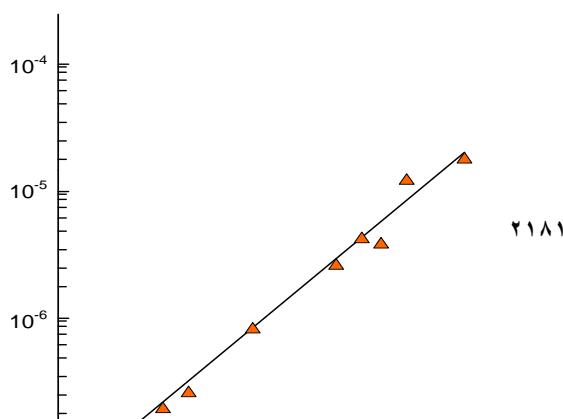
Crack length l (mm)

Figure.(22) Crack growth data (dl/dN vs l relation), Case(1)



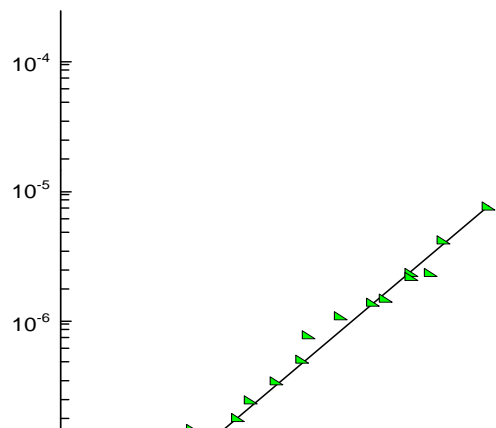
Crack length l (mm)

Figure.(23) Crack growth data (dl/dN vs l relation), Case(2), under stress amplitude 200 MPa



Crack length l (mm)

Figure.(24) Crack growth data (dl/dN vs l relation), Case(2) under stress amplitude 160 MPa



dl/dN mm/cycle

dl/dN mm/cycle

Crack length l (mm)

Crack length l (mm)

Figure.(25) Crack growth data (dl/dN vs l relation), Case(2), under stress amplitude 120 MPa

Figure.(26) Crack growth data (dl/dN vs l relation), Case(2), under stress amplitude 100 MPa

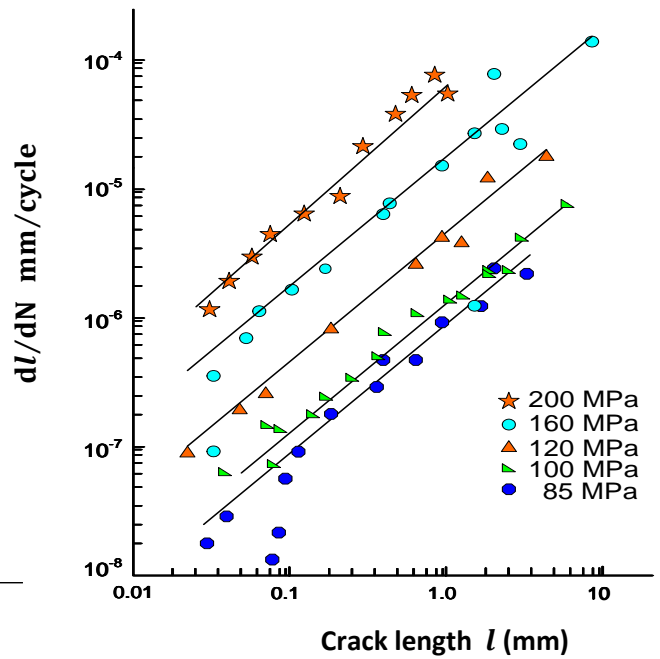
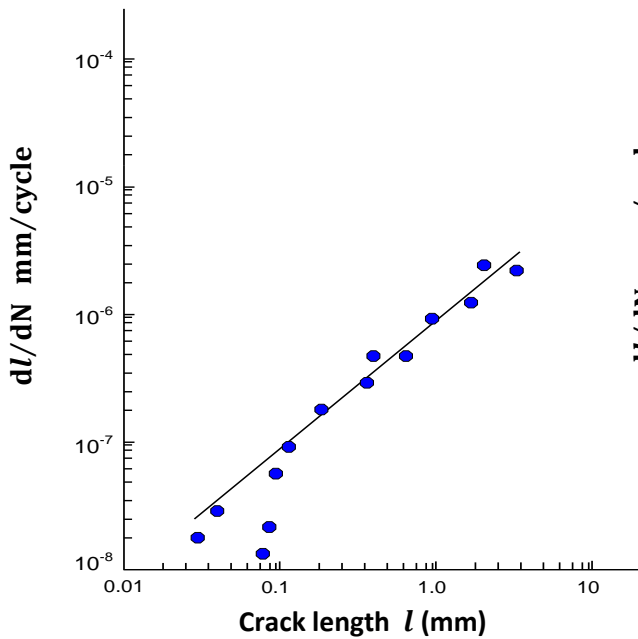
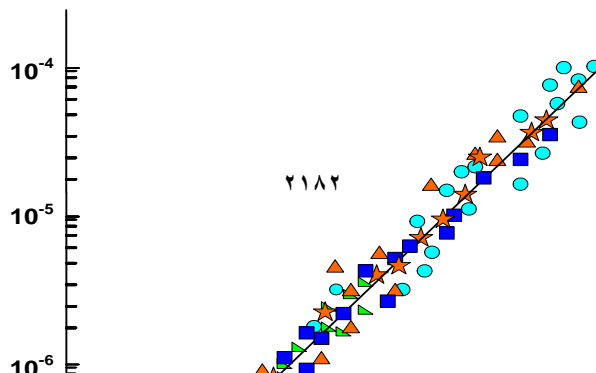


Figure.(27) Crack growth data (dl/dN vs l relation), Case(2), under stress amplitude 85 MPa

Figure.(28) Crack growth data (dl/dN vs l relation), Case(2)



dl/dN mm/cycle

$\sigma_a^n l$ [(MPa)ⁿ (mm)]

Figure.(29) dl/dN vs $\sigma_a^n l$ relation, Case(1)

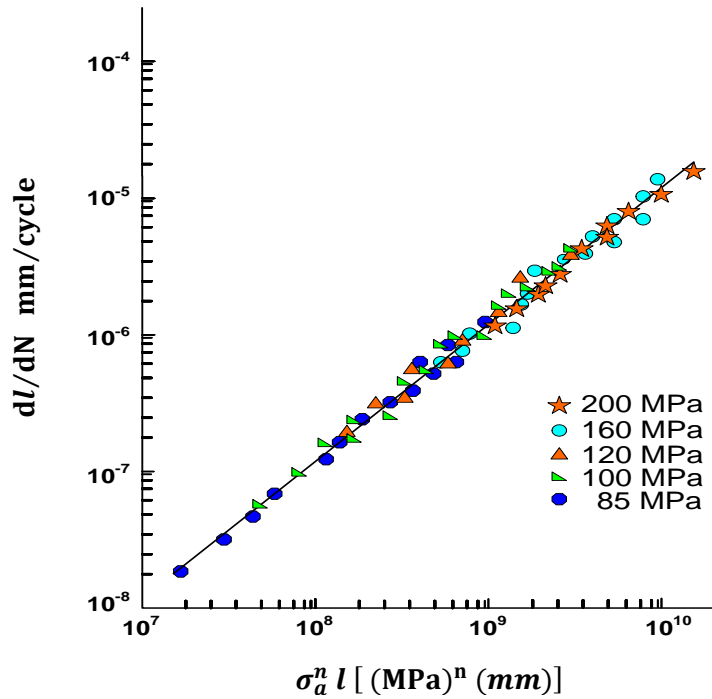


Figure.(30) dl/dN vs $\sigma_a^n l$ relation, Case(2)